^1H and ^{15}N Nuclear Magnetic Resonance Assignments, Secondary Structure in Solution, and Solvent Exchange Properties of Azurin from *Alcaligenes denitrificans*†

Carla W. G. Hoitink,‡ Paul C. Driscoll,§ H. Allen O. Hill,∥ and Gerard W. Canters*,‡

Department of Chemistry, Gorlaeus Laboratories, Leiden University, The Netherlands, Department of Biochemistry, University of Oxford, South Parks Road, Oxford OX1 3QU, United Kingdom, and Department of Inorganic Chemistry, University of Oxford, South Parks Road, Oxford OX1 3QR, United Kingdom

Received July 22, 1993; Revised Manuscript Received November 19, 1993®

ABSTRACT: Complete sequential ^1H and ^{15}N resonance assignments for the reduced Cu(I) form of the blue copper protein azurin (M_r = 14 000, 129 residues) from *Alcaligenes denitrificans* have been obtained at pH 5.5 and 32 °C using homo- and heteronuclear two-dimensional and heteronuclear three-dimensional NMR spectroscopy. Comparison of the resonance assignments for the backbone protons with those of *Pseudomonas aeruginosa* azurin, which is 68% homologous in its amino acid sequence and has a very similar three-dimensional structure, showed a high similarity in chemical shift positions. After adjustment for random coil contributions the mean difference in NH chemical shifts is 0.00 ppm (root mean square width = 0.30 ppm), whereas for C^α protons the mean difference is 0.09 ppm (root mean square width = 0.23 ppm). Characteristic NOE connectivities and $^3J_{HN\alpha}$ values were used to determine the secondary structure of azurin in solution. Two β-sheets, one helix, and nine tight and four helical turns were identified, and some long-range NOE contacts were found that connect the helix with the β-sheets. The secondary structure obtained is in agreement with the structure derived from X-ray diffraction data [Baker, E. N. (1988) *J. Mol. Biol. 203*, 1071–1095]. Studies of the hydration of the protein in the vicinity of the copper ligand residue His117 revealed that the solvent-exposed $N^{\epsilon 2}H$ of His117 is in slow exchange with the bulk solvent. However, no evidence was obtained for the presence of a long-lived water molecule at the position corresponding to a well-defined water molecule observed in the crystal structures of *A. denitrificans* and *Ps. aeruginosa* azurin.

Azurin belongs, together with plastocyanins, pseudo-azurins, and amicyanins, to the family of type I, or blue, copper proteins. Common features within this family are an intense blue color, a relatively high midpoint potential, and a small hyperfine splitting constant in the EPR spectrum. The proteins have been subjected to extensive spectroscopic, kinetic [reviewed by Adman (1985) and Sykes (1991)], and X-ray studies [reviewed by Adman (1991)].

The X-ray structure of azurin shows that the main structural elements of the protein fold are two face-to-face β-sheets (Figure 1). The copper ion is situated at about 7 Å below the protein surface, sandwiched between the two β-sheets. One of the copper ligand residues (His46) is located in one of these sheets. The other three copper ligands (Cys112, His117, and Met121) come from a loop connecting two β-strands in the other β-sheet. A possible fifth coordinating group is the carbonyl of Gly45. This copper-site geometry is best described as trigonal pyramidal or trigonal bipyramidal, depending on the number of ligands (Baker, 1988; Shepard, 1991). Other small blue copper proteins have the same overall architecture (Adman, 1991), and they all appear to function as electron transfer proteins in redox chains.

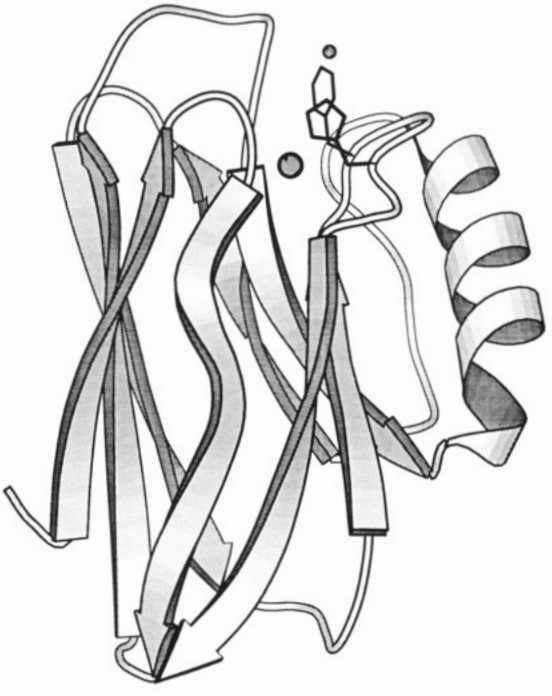

FIGURE 1: Schematic representation of azurin (Kraus, 1991) from *A. denitrificans*. β-Strands are indicated by arrowed ribbons, and the large circle represents the copper ion. Also shown are the side chains of Phe114 and the copper ligand His117, which are within a distance of 4 Å from the well-defined water molecule W137 (small dot) as observed in the crystal structure (see text).

The kinetics of electron transfer of blue copper proteins have been studied for heterogenous as well as homogenous reactions, the latter mainly with NMR spectroscopy (Groeneveld et al., 1988; Groeneveld & Canters, 1988; Armstrong

† This study was supported in part by the Netherlands Foundation for Chemical Research (SON) with financial aid from the Netherlands Organization for Scientific Research (NWO). Support by a NATO travel grant (CRG 900603) to G.W.C. and H.A.O.H. is gratefully acknowledged. P.C.D. is a Royal Society University Research Fellow.

* Address correspondence to this author at Gorlaeus Laboratories, Department of Chemistry, Leiden University, P.O. Box 9502, 2300 RA Leiden, The Netherlands. Telephone: +31-71-274256. Telefax: +31-71-274537.

‡ Leiden University.

§ Department of Biochemistry, University of Oxford.

∥ Department of Inorganic Chemistry, University of Oxford.

® Abstract published in *Advance ACS Abstracts,* January 15, 1994.

0006-2960/94/0433-3560$04.50/0

et al., 1985; Lommen et al., 1990).

Plastocyanin is part of photosystem I and probably uses two surface patches to interact with its redox partners (He et al., 1991; Nordling et al., 1991). Azurin is purported to have a role in anaerobic nitrate respiration and possibly uses only a single surface patch for electron transfer. The electrons enter and leave azurin *via* the copper ligand His117, which is protruding into a shallow pocket on the protein surface (Van de Kamp et al., 1990a,b). In the X-ray structures of *Pseudomonas aeruginosa* and *Alcaligenes denitrificans* azurin this pocket is filled by a highly ordered water molecule which makes H-bonds[1] to the $N^{\epsilon 2}H$ of His117 and the backbone carbonyl group of Ala43 (Baker, 1988; Nar et al., 1991a) and thus could be part of a short through-bond electron pathway from the copper site to the external surface of the protein.

In the last 5 years, a series of azurin mutants have been constructed with the purpose of gaining insight into the relationship between structure and function of blue copper proteins (Van de Kamp et al., 1990b; Den Blaauwen et al., 1993; Karlsson et al., 1991; Hoitink & Canters, 1992; Romero et al., 1993; Canters & Gilardi, 1993). As point mutations usually have localized effects on protein structure and dynamics, information about these effects can be derived from a limited number of NMR experiments. A prerequisite for this type of investigation is a complete assignment of resonances for the wild-type protein.

Complete assignments have already been obtained for several blue copper proteins: plastocyanin from spinach (Driscoll et al., 1987), *Scenedesmus obliquus* (Moore et al., 1988), and french bean (Chazin et al., 1988) and amicyanin from *Thiobacillus versutus* (Lommen et al., 1991). For the latter three, the 3D solution structures also were derived from NMR data (Moore et al., 1988b, 1991; Kalverda et al., 1991). Although the azurins are somewhat bigger (14 kDa), overexpression of their genes in *Escherichia coli* (Karlsson et al., 1989; Van de Kamp et al., 1990c; Hoitink & Canters, 1992) improves the possibility to isotopically enrich these proteins, which facilitates the resonance assignment procedure. Complete assignments for *Ps. aeruginosa* azurin were obtained with 3D ^{1}H homonuclear and 3D ^{1}H[^{15}N] heteronuclear NMR experiments (Van de Kamp et al., 1992). In a previous paper, the assignments of some histidine and methionine resonances were reported for *A. denitrificans* (Groeneveld et al., 1988). Here, all sequential ^{1}H and protonated ^{15}N resonances for this azurin are presented, together with an analysis of the protein's secondary structure derived from the NMR data. We also present the results of an investigation of the hydration of the protein using ROESY spectroscopy and the attempt to identify the residence lifetime of the water molecule in the His117 crevice.

EXPERIMENTAL PROCEDURES

Isolation and ^{15}N Labeling of Azurin. Unlabeled azurin was isolated from *E. coli* JM101 cells transformed with plasmid pCH5, harboring the *A. denitrificans azu* gene on a pUC plasmid (Hoitink & Canters, 1992). Uniformly ^{15}N-labeled azurin was obtained after growth of bacteria on minimal medium with $^{15}NH_4Cl$ (0.5 g/L) (Muchmore et al., 1989), trace elements (1 mL/L) (Light & Garland, 1971), ampicillin (50 μg/mL), and $CuSO_4$ (25 μM) in a fermenter (NBS MPP40, New Brunswick, NJ). Expression of azurin was induced by addition of 0.1 mM IPTG when the optical density was 1.0. After another 5 h of growth, oxygen consumption decreased and the cells were harvested. Azurin was isolated and purified as described before (Hoitink & Canters, 1992). Yields of azurin amounted to ca. 12.5 mg of azurin per liter of bacterial culture for growth on LB medium and varied between 0.3 and 3 mg of azurin per liter for growth on minimal medium.

NMR Sample Preparation. NMR experiments were performed with 2–4 mM reduced Cu(I)-azurin in 20 mM phosphate buffer, pH 6.7 or 5.5, in 90% H_2O/10% D_2O or in 99.95% D_2O. Measurements of pH were not corrected for isotope effects. Two D_2O samples were prepared in the course of the experiments. For one sample 99.95% D_2O was added to Cu(II)-azurin, after which the solution was freeze-dried immediately. This was repeated two times. For the other sample H/D exchange was promoted by incubating oxidized azurin in D_2O at room temperature at pH 8.5 overnight.

Cu(I)-azurin samples were prepared by adding $Na_2S_2O_4$ (0.1 M in 0.1 M NaOH) to a deoxygenated solution of oxidized azurin in an NMR tube. The sample was deoxygenated by carefully alternating evacuation and argon flushing in a closed system. After addition of dithionite this treatment was repeated, and the tube was closed with a tight rubber cap. Azurin samples prepared in this way did not oxidize for at least 2 months.

NMR Spectroscopy. 2D and 3D NMR spectroscopy was performed on NMR spectrometers equipped with Oxford Magnet Ltd. superconducting magnets operating at ^{1}H frequencies of 500.1 and 600.1 MHz. 2D ^{1}H homonuclear experiments in D_2O solution were performed on a Bruker AM600 spectrometer. 2D experiments in H_2O solution were performed on a 600-MHz spectrometer incorporating home-built RF transmitter and receiver components interfaced with a GE/Nicolet Omega computer console. Heteronuclear ^{1}H-[^{15}N] 2D and 3D spectroscopy was performed on a similar hybrid home-built/Omega spectrometer operating at 500.1 MHz (^{1}H) and 50.7 MHz (^{15}N) frequencies. The NMR spectra were all recorded at 32 °C unless stated otherwise.

Homonuclear NMR. The following 2D ^{1}H spectra were recorded in D_2O solution: HOHAHA spectroscopy (Braunschweiler & Ernst, 1983; Davis & Bax, 1985) using a 46-ms WALTZ-17 mixing scheme (Shaka et al., 1983; Bax et al., 1987); NOESY (Jeener et al., 1979; Macura et al., 1981) with a mixing time of 125 ms; and double-quantum filtered COSY spectroscopy (Rance et al., 1983) with phase cycling to suppress repetition rate artifacts [Derome & Williamson, 1990].

The following 2D ^{1}H spectra were recorded in 90% H_2O/10% D_2O solution: a 40-ms mixing time HOHAHA with jump–return read pulse (Plateau & Gueron, 1982) as described by Bax (1989) but with a DIPSI-3 composite pulse mixing period (Shaka et al., 1988); a 150-ms mixing time NOESY with a jump–return read pulse (Driscoll et al., 1989); a phase-sensitive COSY (Aue et al., 1976) with presaturation of the solvent resonance by selective irradiation; and NOESY (110-ms mixing time) and ROESY experiments (50-ms mixing time) (Bothner-By et al., 1984) with selective-pulse water suppression prior to acquisition using the scheme of Gaussian-

[1] Abbreviations: 2D, two dimensional; 3D, three dimensional; COSY, correlation spectroscopy; δ, chemical shift; TSP, (trimethylsilyl)propionic acid; H-bond, hydrogen bond; $d_{xy}(i,i+1)$, NOE between proton X on residue i and proton Y on residue $i+1$; HS(/M)QC, heteronuclear single (/multiple) quantum coherence; HOHAHA, homonuclear Hartmann–Hahn; NOE, nuclear Overhauser effect; NOESY, NOE spectroscopy; ROE, rotating frame Overhauser effect; ROESY, ROE spectroscopy; TPPI, time-proportional phase incrementation; IPTG, isopropyl β-D-thiogalactopyranoside; *azu*, the azurin encoding gene; rmsw, root mean square width.

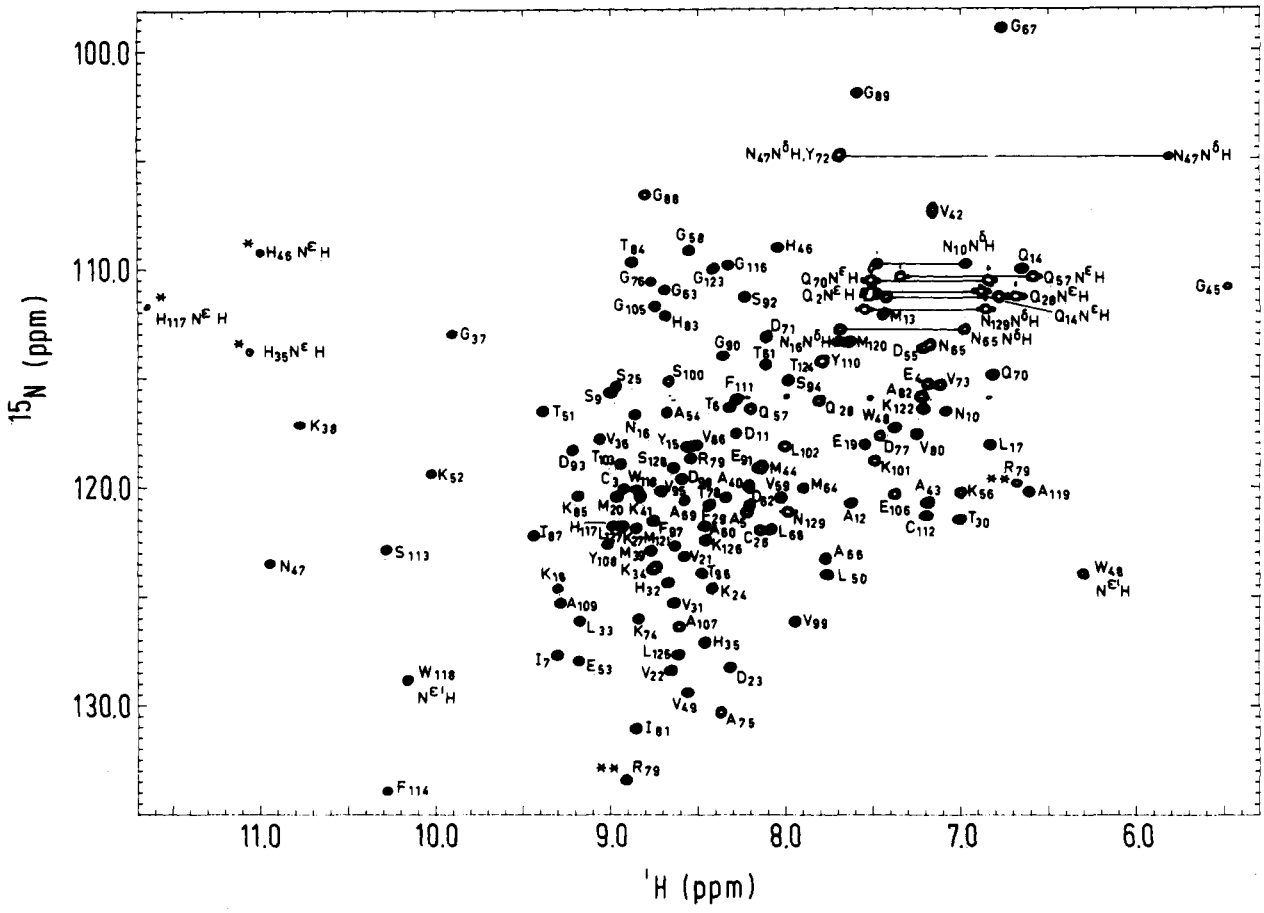

FIGURE 2: Contour plot of the fingerprint region of a 500-MHz ^{1}H[^{15}N] HSQC spectrum of 3 mM ^{15}N-labeled Cu(I)-azurin recorded in 90% H_2O/10% D_2O at pH 5.5 and 32 °C. Assignments of all backbone NH peaks with exception of the first two residues, which were not observed, are labeled. In addition, the side chain NH groups of histidines, amides, and tryptophans are indicated. Folded peaks are indicated with an asterisk; the tentatively assigned side chain protons of Arg79 are indicated with two asterisks.

shaped DANTE selective pulses and a 2-ms spin-lock pulse described by Otting and Wüthrich (1989). The latter two experiments were performed at both 25 and 12 °C.

All spectra were recorded in a phase-sensitive manner using either TPPI or hypercomplex (States) methods for F_1 sign discrimination (Marion & Wüthrich, 1983; States et al., 1982). Where appropriate, States–TPPI was used to place axial peak artifacts at the edge of the 2D spectrum (Marion et al., 1989c). In all these experiments a ^{1}H spectral window of 9009 Hz was used with typically 800–1024 real (or 400–512 complex) t_1 increments, and 16 or 32 transients per t_1 increment.

Heteronuclear NMR. For heteronuclear ^{1}H[^{15}N] NMR spectroscopy the ^{15}N carrier frequency was placed in the middle of the main chain amide region at δ = 116.4 ppm. 2D HSQC spectroscopy (Bax et al., 1990; Norwood et al., 1990) was performed with the $(1/4J)$ delay set to 2.4 ms. A total of 256 t_1 increments were recorded with a ^{15}N spectral window of 2500 Hz. This spectrum was used for the general characterization of the ^{15}N spectrum and allowed the selection of parameters for optimal digital resolution (by folding of outlying ^{15}N resonances) in heteronuclear 3D spectroscopy. For the extraction of coupling constants a 2D ^{1}H[^{15}N] HMQC-J spectrum was recorded with presaturation of the solvent signal (Kay & Bax, 1990).

3D NOESY-HMQC and HOHAHA-HMQC spectra (Kay et al., 1989; Driscoll et al., 1990; Marion et al., 1989a) were recorded with the following parameters: F_3 (^{1}H) 512 complex t_3 data points, 7518 Hz spectral width, ^{1}H carrier at the H_2O frequency; F_2 (^{15}N) 32 complex t_2 points, 1204 Hz spectral width; F_1 (^{1}H) 128 complex t_1 points, 6451 Hz spectral width. The mixing times in the 3D NOESY-HMQC and HOHAHA-HMQC spectra were 125 and 33 ms, respectively. Low-power irradiation of the H_2O resonance combined with spin-lock purge pulses was used to suppress the solvent signal in both 3D experiments (Messerle et al., 1989). States-TPPI sign discrimination was used in the F_1 and F_2 dimensions, with initial t_1 and t_2 delays set to obtain distortionless baselines and pure absorption mode line shapes for folded peaks (Bax et al., 1991). The 3D spectra were zero-filled once in each dimension prior to Fourier transformation yielding a final real absorption mode matrix with the dimensions 512 (F_3) × 64 (F_2) × 256 (F_1) data points. 3D NOESY-HMQC and HOHAHA-HMQC spectra were recorded on a sample of azurin at pH 6.7 with an additional 3D NOESY-HMQC spectrum at pH 5.5. Two dummy scans and eight transients per t_1 and t_2 increment were performed, the recycle time was 1.6 s, and the duration of each 3D experiment was ca. 3 days.

Data Processing. All data were processed on a SUN Sparc workstation using the program Felix 1.1 (Hare Research Inc.). For all 2D experiments except COSY, the data were zero-filled in the F_2 dimension, apodized with a Lorentz-to-Gaussian function, Fourier transformed, and baseline corrected. For the F_1 dimension, the data were multiplied with a 60°-shifted squared sine-bell apodization function, Fourier transformed, and interactively phase corrected. Unshifted sine-bell window functions were used for processing both dimensions of the COSY and double-quantum filtered COSY data. Data acquired in water were first deconvoluted in the time domain with a Gaussian function prior to Fourier transformation in F_2 (Marion et al., 1989b).

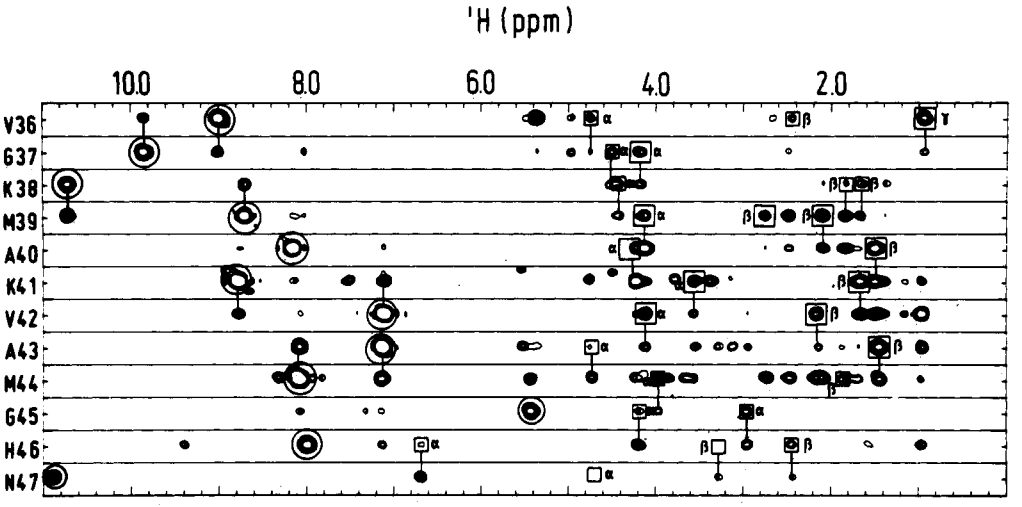

FIGURE 3: F_1/F_3 ^{1}H/^{1}H contour slices containing ^{15}NH-NOESY lines from the 3D ^{1}H[^{15}N] NOESY-HMQC spectrum at the respective F_2 positions of the ^{15}N chemical shifts of residues Val36–Asn47. The main-chain ^{15}NH HMQC peaks are circled and intraresidue NOE connectivities are boxed. Sequential NOEs are indicated by solid lines between slices.

$^3J_{HN\alpha}$ coupling constants were derived by numerical nonlinear least-squares line-shape fitting of t_1 cross sections from the HMQC-J experiment as described previously (Norwood et al., 1992).

^{1}H chemical shift calibration was performed with TSP. ^{15}N chemical shifts were calculated relative to the ^{1}H standard with the calibrated frequency ratio ^{15}N/^{1}H (Live et al., 1984). Quoted ^{1}H chemical shifts are referenced to TSP, and ^{15}N chemical shifts are relative to liquid ammonia.

RESULTS

The concepts behind the sequential resonance assignments and the identification of secondary structure elements are described by Wüthrich (1986).

Sequence-Specific Assignments. ^{15}N-labeled azurin was used for heteronuclear 2D and 3D NMR spectroscopy. The dispersion of the peaks in the 2D HSQC spectrum was good, facilitating the analysis of the 3D spectra (Figure 2). There are only two instances of severe cross peak overlap in the HSQC spectrum, both involving the superposition of a backbone NH signal with one of the cross peaks from a asparagine side chain NH_2 group, i.e., the NH of Tyr72 with an NH_2 peak of Asn47 and the NH of Met120 with an NH_2 peak of Asn16 (Figure 2). Sequence-specific resonance assignments were obtained by analysis of the 3D NOESY-HMQC and HOHAHA-HMQC spectra. These spectra were visualized by plotting slices through the ^{15}N (F_2) frequency along the proton axes (F_1 and F_3) (Driscoll et al., 1990) as shown for the residues Val36–Asn47 in Figure 3. Discrimination between intraresidue and interresidue NOEs was obtained by overlaying the 3D HOHAHA-HMQC spectrum with the 3D NOESY-HMQC spectrum. In the 3D HOHA-HA-HMQC spectrum it was possible to detect connectivities from at least one β-proton to each backbone amide NH. Analysis of 2D ^{1}H HOHAHA spectra recorded in D_2O solution at two temperatures allowed identification of spin system types. The unique valine, alanine, threonine, and glycine spins systems provided good starting points for the sequential assignments. No NH resonances could be observed in the pH 6.7 spectra for the following seven residues: Ala1, Gln2, Cys3, Lys18, Lys27, Ala69, and Gly76. This is probably due to fast exchange of these NH groups with the solvent at the pH used in the experiments. The recording of an additional 3D NOESY-HMQC spectrum at a lower pH (5.5) allowed for the identification of all backbone amide resonances, with the exception of the first two residues in the amino acid sequence. The sequential assignements were derived almost exclusively via $d_{\alpha N}(i,i+1)$ [or $d_{\alpha\delta}(i,i+1)$ for the prolines] NOE connectivities, with exception of three contacts that could not be observed due to overlap, as summarized in Figure 4. For all three exceptions, sequential NOE contacts, $d_{NN}(i,i+1)$, were observed between NH protons.

Chemical Shifts. A plot of the chemical shifts corrected for random coil contributions (Wishart et al., 1991) versus the amino acid sequence for the NH and C$^\alpha$H protons of azurin is shown in Figure 5a,b. The corresponding chemical shift profile of the homologous *Ps. aeruginosa* azurin is included for comparison. The NMR data for *Ps. aeruginosa* azurin have been acquired at the same pH and buffer as for *A. denitrificans* azurin, only at a higher temperature, i.e., at 40 instead of 32 °C (Van de Kamp et al., 1992). This temperature difference has an effect of less than 0.015 ppm on the chemical shifts of azurin (data not shown); differences in chemical shifts between the two azurins that are larger than 0.015 ppm therefore reflect differences in ring current effects, secondary structure, or electrostatic effects (Williamson & Asakura, 1991). Differences in individual backbone chemical shifts between the two azurins are greater than 0.5 ppm for only 17 protons (Figure 5c,d). It has been shown that chemical shifts of NH and C$^\alpha$H protons exhibit a strong correlation with the local secondary structure (Wishart et al., 1991). The overall high similarity in chemical shifts of the backbone protons of azurin from *A. denitrificans* with those of *Ps. aeruginosa* azurin, which has 68% identity in primary structure and is essentially identical in secondary structure as assessed both by X-ray crystallography and NMR, is in accordance with that study.

The mean difference in chemical shift for the NH protons is 0.00 ppm with a rmsw of 0.30 ppm. The mean difference in chemical shift for the C$^\alpha$H protons between *A. denitrificans* and *Ps. aeruginosa* azurin is 0.09 ppm with a rmsw of 0.23 ppm.

Spin System Assignments. Following completion of the sequential assignment of the backbone resonances in the 3D spectra, complete side chain assignments were made from 2D COSY, HOHAHA, and NOESY spectra. Resonances were observed for all asparagine N$^{\delta}$H$_2$ and glutamine N$^{\epsilon}$H$_2$ side chain protons, for the N$^{\epsilon 2}$H protons of His35, His46, and

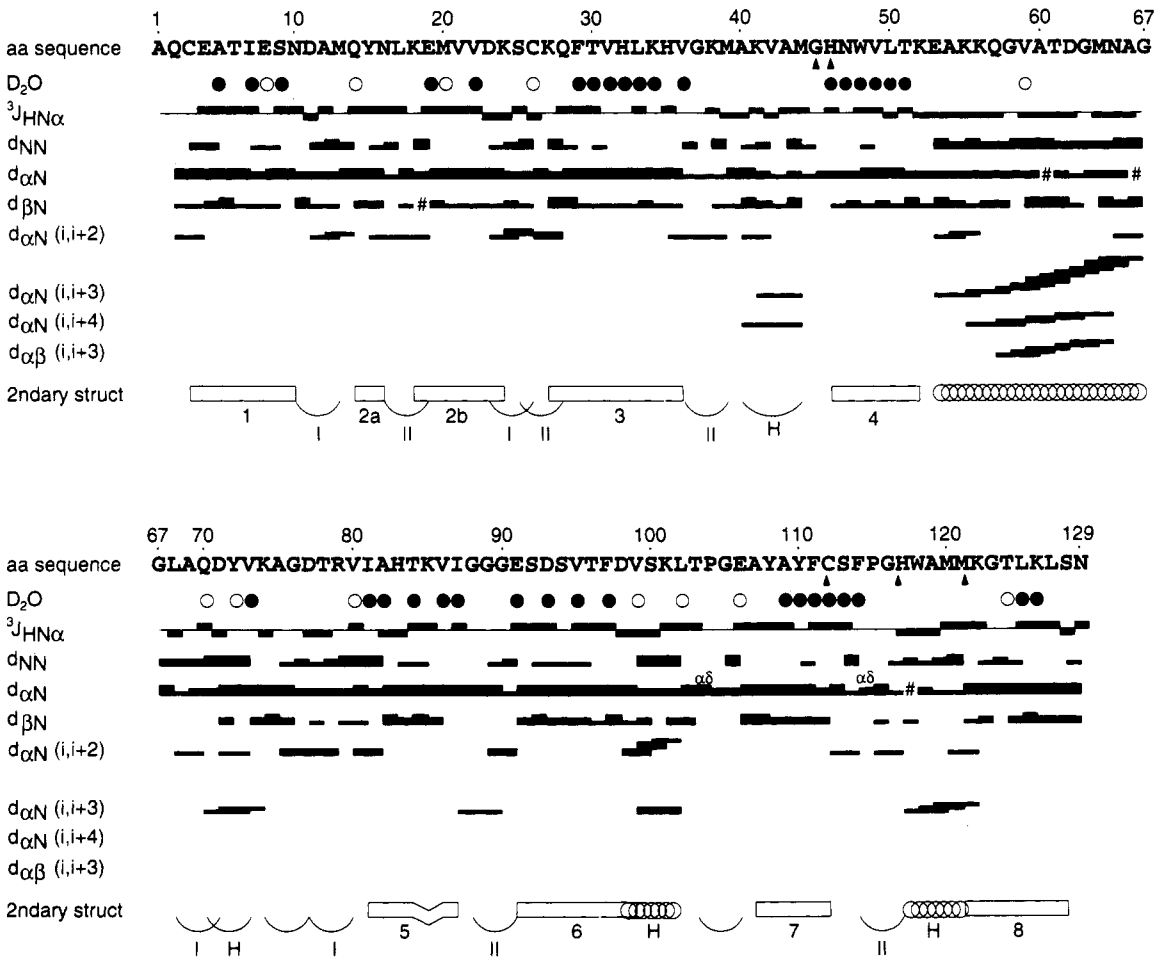

FIGURE 4: Collection of observed short- and medium-range sequential NOEs. Intensities were derived from HMQC-NOESY and NOESY spectra with a mixing time of 125 ms and classified relative to the number of contour levels. The upper line shows the amino acid sequence with the copper ligands marked by a triangle, the second line indicates the residues whose NH–C$^{\alpha}$H cross peaks are observed in correlation spectra for azurin in D_2O and whose NHs thus exchange very slowly (time scale of hours to days). Closed circles represent peaks that are observed in both samples, i.e., one prepared by freeze-drying and the other one by incubating azurin overnight in D_2O; open circles represent peaks that were observed in the sample prepared by freeze-drying only. The third line contains $^3J_{HN\alpha}$ values derived from a HMQC-*J* spectrum (lower bars <6 Hz, raised bars >6 Hz). Absence of a bar means not determined. A # mark in the lines indicates that the determination of the cross peak was hindered by overlap. In the bottom line, secondary structure elements are denoted. Turns have been classified according to Wüthrich (1986). The numbers of the β-strands (open boxes) refer to the numbering from the crystal structure (Baker, 1988); turns are denoted by I, II, or H, i.e., type I, type II, or helical turn, respectively. The helix is indicated by an array of overlapping circles. The kink in strand 5 represents a β-bulge.

His117 and for the O$^{\gamma 1}$H, O$^{\gamma 1}$H, O$^{\gamma}$H, and O$^{\eta}$H of Thr51, Thr84, Ser113, and Tyr110, respectively. Also the indole N$^{\epsilon 1}$H protons of Trp48 and Trp118 could be readily identified. Met C$^{\epsilon}$H$_3$ protons were identified by the observation of $d_{\epsilon\beta}(i,i)$ NOEs, except for Met64 and Met120. Two folded cross peaks in the ^{1}H[^{15}N] HSQC spectrum probably arise from the side chain of the unique arginine residue Arg79 but could not be unambiguously assigned because of insufficient relayed coherence transfer. The aromatic ring of the Tyr110 side chain is found to be slowly flipping at the NMR time scale, which enables observation of four resolved aromatic resonances for this residue. Broadening of the aromatic proton resonances of Tyr72 and Phe114 indicates that these rings are flipping at an intermediate rate.

Out of the total of 129 residues, complete ^{15}N and ^{1}H resonance assignments were obtained for 102 residues and partial ^{1}H assignments for the remaining 27 residues, which include 12 lysine side chains with overlapping cross peaks. The resonance assignments are listed in Table 1.

Secondary Structure. The recognition and definition of secondary structure elements was based on intra- and interresidue NOE connectivities and $^3J_{HN\alpha}$ values derived from a HMQC-*J* experiment. The coupling constants are given in Table 1 and are qualitatively represented in Figure 4.

The secondary structure of azurin as derived from the NMR data contains two β-sheets, one helix, nine tight and four helical turns (Figures 4 and 5). The turn types between residues Val73 and Asp77 and between Thr103 and Glu106 could not be determined from the available NMR data and are therefore designated simply as "turn" in Figure 4.

The two β-sheets are connected at one side by β-strand 2, which exhibits a turn in the middle. No NOE contacts were found at the other side of the β-sheet between strands 5 and 6. A few NOE contacts indicate packing of the helix against the β-sheets: a contact from the C$^{\alpha}$H of Asp71 to the NH of Val86, and a contact between the C$^{\alpha}$H from Gly63 to the NH of Lys74 and the C$^{\alpha}$H of Val73.

Proton Solvent Exchange. Slowly exchanging backbone amide protons of azurin were identified by the observation of NH–C$^{\alpha}$H cross peaks in the COSY and HOHAHA spectra that were recorded in D_2O solution. Thirty-six peaks were observed at pH 6.7 after allowing exchange of NH protons overnight, and 48 were observed after the short contact freeze-drying cycles (Figure 4). Most of the main-chain NH protons

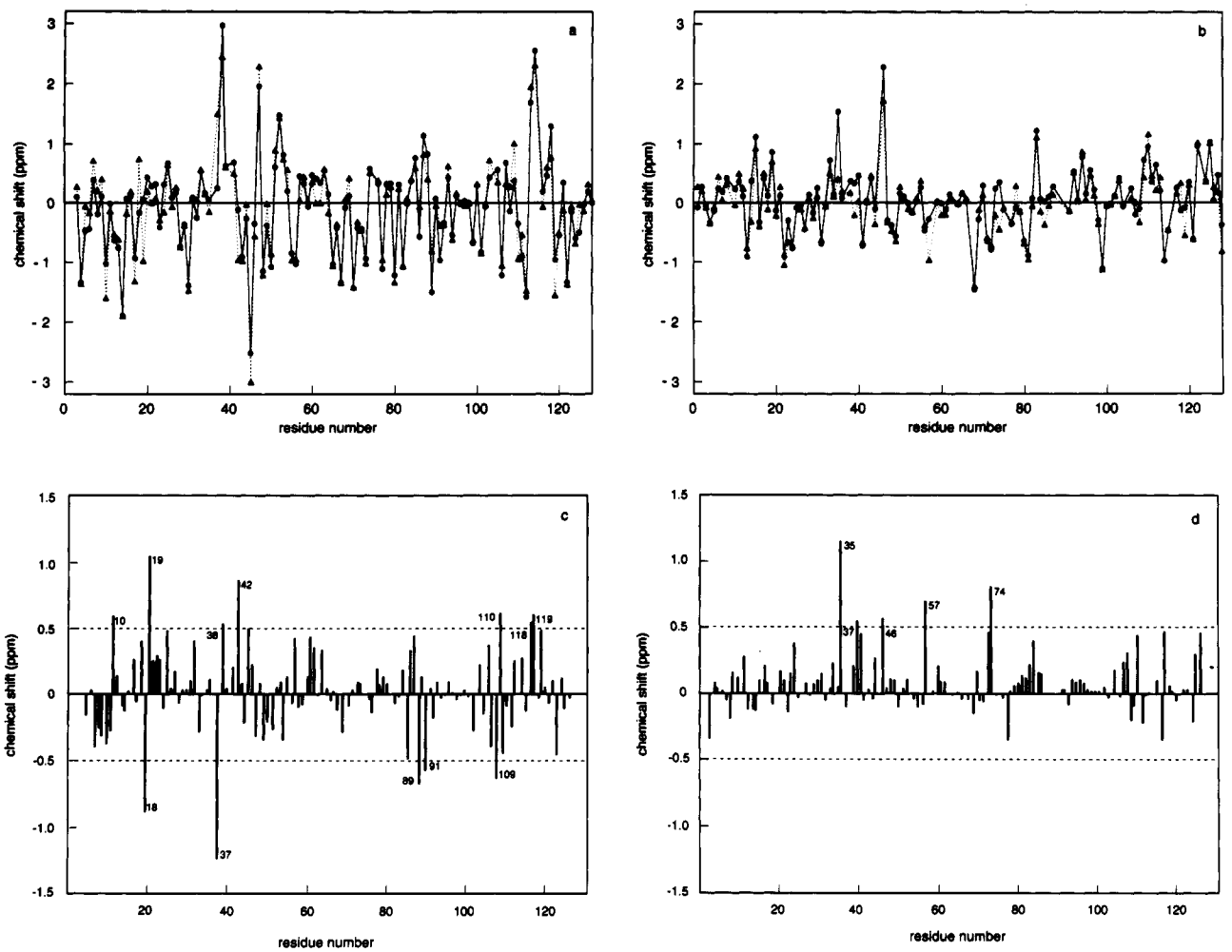

FIGURE 5: (a, b) Comparison of chemical shifts of NH (a) and C$^\alpha$H (b) protons between azurin from *Ps. aeruginosa* (solid line, circles) and *A. denitrificans* (dashed line, triangles). Chemical shifts have been corrected for random coil values. Shown are chemical shifts for the NH protons of residues 3–128 with exception of the positions where a proline occurs in either of the azurins and for the C$^\alpha$H protons between residues 1–128 with exception of the positions where a glycine is found in either of the azurins. (c, d) Differences in chemical shift positions between NH (c) and C$^\alpha$H (d) protons from *Ps. aeruginosa* and *A. denitrificans* azurin, corrected for random coil values. Open bars represent identical amino acids; closed bars different amino acids. Glycine C$^\alpha$H protons are not included. The numbers refer to the positions in the amino acid sequence.

observed under these conditions occur in central β-strands or at the expected positions at the end of turns. Also visible are the NH protons of Ser113 and Phe114, which are part of the structural motif of the copper site and which in the crystal structure are involved in several H-bonds.

In order to investigate the hydration of the protein in solution, a series of 2D ^{1}H NOESY and ROESY experiments were performed. By using shaped-pulse selective suppression of the water resonance (Otting & Wüthrich, 1989), it is possible to obtain spectra containing NOE cross-peak connectivities from both labile and nonlabile protons to the solvent resonance. The advantage of using shaped-pulse water suppression over the jump–return method (Plateau & Gueron, 1982) is that in the final step of the first pulse sequence essentially uniform excitation of the ^{1}H spectrum is obtained (apart from a small region immediately adjacent to the solvent resonance).

In a NOESY spectrum, a cross peak occurring at the H_2O resonance frequency may be due to (1) cross-relaxation between a protein proton and a nearby proton from a water molecule with a long residence lifetime (compared to the rotational correlation time of the protein molecule), (2) cross-relaxation of a protein proton and another solvent-exchangeable proton in the protein having a solvent exchange-averaged chemical shift, or (3) in the case of a labile NH or OH, chemical exchange of the proton directly with the solvent. In a ROESY spectrum it is possible to distinguish cross-relaxation effects from solvent exchange according to the sign of the cross peaks at the H_2O frequency (Otting & Wüthrich, 1989; Clore et al., 1990). When the diagonal peaks of the azurin ROESY spectrum are phased in the negative sense, cross-relaxation effects (i.e., NOEs) give rise to positive cross peaks, whereas chemical exchange of exchangeable protons with H_2O is manifested by negative cross-peaks.

110-ms NOESY and 50-ms ROESY experiments were performed on a 4 mM sample of azurin at both 12 and 25 °C. An example of the results obtained is shown in Figure 7 which illustrates the region downfield of the water resonance in the ROESY spectrum obtained at 25 °C. The spectrum shows that there are a number of cross peak connectivities between protons in the protein and solvent protons. A 1D cross section taken at the frequency of the water resonance (parallel to the F_2 axis) is also shown in Figure 7. Eleven resolved peaks were observed in the region between 5 and 12 ppm. The cluster of negative peaks around 7.5 ppm represents exchange of side chain amide groups with solvent. The peak at 9.9 ppm has been assigned to a NOE between the NH proton of Lys52 and its C$^\alpha$H proton, which has the same chemical shift as water at this temperature. Four cross peaks at 6.48, 6.81, 6.74, and 7.24 ppm can be accounted for by NOEs from aromatic protons of histidines and tyrosines. They originate from indirect

Table 1: ^{15}N and ^{1}H Chemical Shifts (ppm) for Reduced Azurin from *A. denitrificans* at pH 5.5 and 32 °C, in 20 mM Potassium Phosphate Buffer[a]

residue	$^{3}J_{HN\alpha}$	$^{15}N(H)$	$(N)^{1}H$	$C^{\alpha}H$	$C^{\beta}H$	other ^{1}H (^{15}N)
Ala 1				4.46	1.33	
Gln 2				4.47	2.18, 2.08	$C^{\gamma}H$ 2.46; $N^{\epsilon 2}H$ 7.51, 6.88 (111.5)
Cys 3		120.5	8.88	5.01	4.11, 2.75	
Glu 4	6.8	115.7	7.12	4.49	1.47, 1.68	*$C^{\gamma}H$ 1.88, 1.84*
Ala 5	7.7	121.6	8.18	4.58	1.32	
Thr 6	13.4	116.8	8.26	5.28	3.85	$C^{\gamma 2}H_3$ 1.03
Ile 7	8.8	128.1	9.28	4.64	1.15	$C^{\gamma 2}H_3$ 0.33; $C^{\gamma 1}H$ 1.64, 0.93; $C^{\delta}H_3$ 0.25
Glu 8		124.1	8.68	5.15	1.64, 1.90	$C^{\gamma}H$ 2.30
Ser 9	8.8	116.1	8.95	5.46	3.36, 3.08	
Asn 10	8.8	116.9	7.01	4.98	2.69, 3.44	$N^{\delta 2}H$ 7.48, 6.97 (110.2)
Asp 11	5.5	118.0	8.23	5.11	3.09, 2.58	
Ala 12	9.2	121.2	7.58	4.43	1.21	
Met 13		112.5	7.40	3.54	2.01, 1.88	$C\gamma H$ 1.77, 1.72; $C^{\epsilon}H_3$ 1.87
Gln 14	8.9	110.4	6.60	4.55	1.68, *1.90*	*$C^{\gamma}H$ 2.18*, 2.26; $N^{\epsilon 2}H$ 7.42, 6.78 (111.7)
Tyr 15		118.6	8.50	5.94	3.16, 3.04	$C^{\delta}H$ 7.03; $C^{\epsilon}H$ 6.55
Asn 16	6.4	117.1	8.80	4.62	3.13, 2.76	$N^{\delta 2}H$ 7.64, 7.57 (113.8)
Leu 17	8.7	118.5	6.78	4.84	1.55, 1.68	$C^{\gamma}H$ *1.73*, $C^{\delta}H_3$ *0.96*
Lys 18		124.8	9.28	4.60	2.10, 1.92	*3.07, 1.63, 1.55*
Glu 19	7.3	118.5	7.50	5.54	1.99, 1.91	$C^{\gamma}H$ 2.10, 2.08
Met 20	9.0	120.9	8.90	4.65	1.92, 1.74	$C\gamma H$ 2.47, 2.28; $C^{\epsilon}H_3$ 1.40
Val 21	9.0	123.6	8.53	4.82	1.88	$C^{\gamma}H_3$ 0.82, 0.71
Val 22	8.6	128.8	8.60	3.50	1.48	$C^{\gamma}H_3$ 0.34, –0.30
Asp 23	2.4	128.7	8.26	4.39	3.05, 2.66	
Lys 24	2.5	125.0	8.38	3.98	1.91, 1.78	*1.19*
Ser 25	7.2	115.8	8.93	4.30	3.88, 3.81	
Cys 26	5.3	122.4	8.10	4.40	3.30, 2.98	
Lys 27		122.3	8.80	4.28	1.88, 1.79	*2.98, 1.54, 1.44*
Gln 28	8.3	116.5	7.75	4.94	1.68	*2.21, 2.12*; $N^{\epsilon 2}H$ 7.52, 6.68 (111.7)
Phe 29	8.7	121.2	8.39	4.81	1.58, 1.49	$C^{\delta}H$ 6.73; $C^{\epsilon}H$ 7.16; $C^{\zeta}H$ 6.96
Thr 30	9.1	121.9	6.95	4.95	3.25	$C^{\gamma 2}H_3$ 0.32
Val 31		125.7	8.59	3.92	0.88	$C^{\gamma}H_3$ 0.16, –0.75
His 32		124.8	8.61	4.90	3.33, 2.87	$C^{\delta 2}H$ 6.74; $C^{\epsilon 1}H$ 8.17
Leu 33	8.2	126.5	9.13	5.18	1.89	$C^{\gamma}H$ 1.44; $C^{\delta}H_3$ 0.94, 0.90
Lys 34		124.2	8.69	4.81	1.55, 1.87	*1.95*
His 35	8.7	127.5	8.41	5.36	3.64, 2.43	$C^{\delta 2}H$ 7.12; $C^{\epsilon 1}H$ 8.03; $N^{\epsilon 2}H$ 11.06 (163.5)
Val 36		118.2	9.00	4.74	2.64	$C^{\gamma}H_3$ 0.91, 0.91
Gly 37		113.4	9.85	4.50, 4.19		
Lys 38	9.4	117.5	10.73	4.39	1.83, 1.64	
Met 39	4.7	123.3	8.71	4.10	2.74, 2.06	$C\gamma H$ 2.43, 1.80; $C^{\epsilon}H_3$ 2.04
Ala 40	4.3	120.4	8.16	4.21	1.46	
Lys 41	8.1	120.8	8.78	3.55	1.63	*1.69, 1.38, 1.15*
Val 42	4.1	107.7	7.11	4.11	2.17	$C^{\gamma}H_3$ 0.94, 0.94
Ala 43	9.6	121.1	7.13	4.65	1.40	
Met 44	7.1	119.5	8.08	3.95	1.84	*1.70, 2.47*; $C^{\epsilon}H_3$ 2.03
Gly 45		111.3	5.43	4.19, 2.95		
His 46	8.9	109.4	8.00	6.68	3.25, 2.42	$C^{\delta 2}H$ 5.43; $C^{\epsilon 1}H$ 6.86; $N^{\epsilon 2}H$ 11.0 (158.9)
Asn 47		123.9	10.90	4.69	2.73, 2.40	$N^{\delta 2}H$ 7.65, 5.76 (105.2)
Trp 48	8.2	117.7	7.33	4.51	3.19, 2.85	$C^{\delta 1}H$ 6.31; $N^{\epsilon 1}H$ 6.26 (124.4); $C^{\epsilon 3}H$ 7.26; $C^{\zeta 2}H$ 6.73; $C^{\zeta 3}H$ 6.35; $C^{\eta 2}H$ 6.66
Val 49	8.7	129.8	8.51	3.90	0.67	$C^{\gamma}H_3$ 0.67, 0.47
Leu 50	5.8	124.4	7.71	4.95	1.25, 0.52	$C^{\gamma}H$ 1.04; $C^{\delta}H_3$ 0.81, 0.10
Thr 51	7.9	116.9	9.32	4.91	4.55	$C\gamma 2H_3$ 1.23; $O^{\gamma 1}H$ 3.95
Lys 52	5.8	119.8	9.98	4.60	1.92, 1.74	*1.87, 1.69*
Glu 53	2.1	128.4	9.13	3.83	1.90	*2.14, 2.34*
Ala 54	3.2	117.0	8.63	4.11	1.34	
Asp 55	8.7	114.1	7.18	4.81	2.85, 2.55	
Lys 56	0.9	120.7	6.95	3.56	1.40, 118	*0.59, 0.02*
Gln 57	0.3	116.8	8.14	3.04	2.03, 1.80	$N^{\epsilon 2}H$ 7.34, 6.59 (110.8)
Gly 58		109.6	8.50	3.65, 3.61		
Val 59	3.8	120.9	7.98	3.58	2.08	$C^{\gamma}H_3$ 1.01, 0.87
Ala 60	3.5	122.2	8.42	3.83	0.46	
Thr 61	4.4	114.8	8.08	3.81	4.17	$C^{\gamma 2}H_3$ 1.17
Asp 62	4.0	163.3	8.15	4.50	2.59, 2.47	
Gly 63		111.4	8.63	4.01, 3.40		
Met 64	2.6	120.5	7.85	4.05	2.50, 2.30	
Asn 65	6.3	113.9	7.13	4.56	2.86, 2.74	$N^{\delta 2}H$ 7.63, 6.93 (113.2)
Ala 66	3.5	123.7	7.71	4.11	1.33	
Gly 67		99.4	6.71	4.12, 3.53		
Leu 68	2.6	122.4	8.03	2.94		
Ala 69		121.0	8.53	4.07	1.38	
Gln 70	9.8	115.3	6.76	4.40	1.40, 2.35	$C^{\gamma}H$ 2.79, 2.14; $N^{\epsilon 2}H$ 7.50, 6.84 (111.0)
Asp 71	5.9	113.5	8.05	4.03	3.00, 2.91	
Tyr 72		105.2	7.63	3.70	3.12, 2.24	$C^{\delta}H$ 7.0; $C^{\epsilon}H$ 6.48
Val 73	8.1	115.7	7.05	3.89	1.30	$C^{\gamma}H_3$ 0.57, 0.26
Lys 74	3.9	126.5	8.79	3.77	1.75, 1.43	*1.24*
Ala 75		130.7	8.33	4.10	1.33	

Table 1 (Continued)

residue	$^3J_{HN\alpha}$	^{15}N(H)	(N)^{1}H	C$^\alpha$H	C$^\beta$H	other ^{1}H (^{15}N)
Gly 76		111.0	8.73	3.91, 3.70		
Asp 77	2.9	118.1	7.41	4.30	2.85, 2.73	
Thr 78	5.4	120.9	8.30	4.64	4.15	C$^\gamma$2H$_3$ 1.35
Arg 79		119.1	8.49	4.16	1.77	*8.91* (*83.2*), *6.63* (*69.8*); C$^\gamma$H 2.85; C$^\delta$H 3.33
Val 80	7.3	118.0	7.19	3.86	2.14	C$^\gamma$H$_3$ 0.78, 0.74
Ile 81		131.5	8.81	3.64	1.10	C$^\gamma$1H 1.60, 1.03; C$^\gamma$2H$_3$ 0.41; C$^\delta$1H$_3$ 0.72
Ala 82	5.6	116.3	7.17	4.60	1.14	
His 83	5.7	112.5	8.63	6.07	3.38, 3.23	C$^{\delta 2}$H 7.24; C$^{\epsilon 1}$H 8.81
Thr 84	8.5	110.1	8.83	4.69	5.21	Cγ2H$_3$ 1.24; O$^\gamma$1H 5.2
Lys 85	6.4	120.8	9.13	4.34	1.56, 1.49	
Val 86		118.5	8.46	4.50	2.09	C$^\gamma$H$_3$ 1.12, 0.98
Ile 87	9.6	122.7	9.39	4.73		*2.19, 0.76*
Gly 88		107.0	8.75	4.11, 3.35		
Gly 89		102.4	7.54	2.48, 2.44		
Gly 90		114.4	8.30	4.23, 3.81		
Glu 91	9.0	119.5	8.10	4.70	2.72	
Ser 92	7.4	111.7	8.18	5.46	3.82, 3.78	
Asp 93	6.4	118.7	9.17	5.08	2.81, 2.21	
Ser 94		115.5	7.93	5.81	3.45, 3.38	
Val 95		120.6	8.69	4.60	1.83	C$^\gamma$H$_3$ 1.05, 0.78
Thr 96	8.7	124.4	8.43	5.31	3.59	C$^\gamma$2H$_3$ 0.91
Phe 97	8.6	121.9	8.72	5.19	3.02, 2.86	C$^\delta$H 6.80; C$^\epsilon$H 6.87; C$^\zeta$H 6.76
Asp 98	5.1	120.0	8.55	4.70	2.88, 2.63	
Val 99	5.1	126.6	7.90	3.42	1.84	C$^\gamma$H$_3$ 0.83, 0.46
Ser 100	4.4	115.5	8.61	4.32	4.01, 3.93	
Lys 101	6.6	119.2	7.43	4.19	1.80	*1.90, 1.63*
Leu 102	8.2	118.5	7.95	4.45	1.96, 1.05	C$^\gamma$H 1.44; C$^\delta$H$_3$ 0.59, –0.13
Thr 103	7.5	119.4	8.88	4.74	4.05	C$^\gamma$2H$_3$ 1.31
Pro 104				4.30	2.37, 1.93	C$^\gamma$H 2.14; C$^\delta$H 4.00, 3.80
Gly 105		112.1	8.70	4.23, 3.68		
Glu 106	7.6	120.7	7.33	4.30	1.82	*1.68*
Ala 107	7.8	126.8	8.56	4.67	1.30	
Tyr 108	8.8	123.2	8.95	4.69	3.05, 2.97	C$^\delta$H 6.95; C$^\epsilon$H 6.81
Ala 109	8.6	125.7	9.25	5.09	1.40	
Tyr 110		114.6	7.73	6.18	1.88, 1.44	Cδ1H 6.63; C$^{\epsilon 1}$H 6.53; C$^{\delta 2}$H 6.46; C$^{\epsilon 2}$H 6.06; O$^\zeta$H 5.5
Phe 111		116.4	8.23	5.52	3.53, (3.28)	C$^\delta$H 6.71; C$^\epsilon$H 7.03; C$^\zeta$H 6.83
Cys 112	9.5	121.7	7.13	5.30	3.12, 2.95	
Ser 113	9.1	123.3	10.24	4.80	4.59, 3.58	O$^\gamma$H 5.75
Phe 114		134.3	10.23	3.45	2.80, 2.28	C$^\delta$H 6.32; C$^\epsilon$H 7.32; C$^\zeta$H 7.13
Pro 115				3.86	1.58, 1.84	C$^\gamma$H 1.41; C$^\delta$H 3.86, 3.18
Gly 116		110.3	8.28	4.37, 3.53		
His 117	4.8	122.2	8.95	4.74	3.76, 3.34	C$^{\delta 2}$H 6.72; C$^{\epsilon 1}$H 7.00; N$^{\epsilon 2}$H 11.65 (161.4)
Trp 118	2.4	120.5	8.79	4.74	3.76, 3.09	C$^{\delta 1}$H 7.47; N$^{\epsilon 1}$H 10.10 (129.3); C$^{\epsilon 3}$H 7.02; C$^{\zeta 2}$H 7.35; C$^{\zeta 3}$H 6.79; C$^{\eta 2}$H 6.98
Ala 119	4.8	120.7	6.56	3.64	0.81	
Met 120	9.9	113.7	7.60	4.61	1.98, 2.33	C$^\gamma$H 2.55, 2.46
Met 121	8.1	123.1	8.58	4.25	1.895	*2.08*; C$^\epsilon$H$_3$ 0.47
Lys 122	8.3	116.8	7.16	5.73	2.15, 2.00	
Gly 123		110.4	8.36	4.21, 3.11		
Thr 124		114.6	7.74	5.19	3.99	C$^\gamma$2H$_3$ 1.25
Leu 125	8.6	128.1	8.54	5.69	1.72, 1.49	C$^\gamma$H 1.51; C$^\delta$H$_3$ 0.94, 0.55
Lys 126	8.1	122.9	8.40	4.97	1.94, 1.75	*1.52, 1.61*
Leu 127	6.4	122.2	8.88	4.86	1.64, 1.50	C$^\gamma$H 1.64; C$^\delta$H$_3$ 0.74
Ser 128	4.2	119.5	8.59	4.13	3.70	
Asn 129	7.8	130.5	7.94	4.48	2.76, 2.65	N$^{\delta 2}$H 7.50, 6.80 (112.3)

[a] ^{1}H chemical shifts (±0.02 ppm) are expressed relative to TSP; ^{15}N chemical shifts (±0.2 ppm) are referred to liquid ammonia. Chemical shifts in italics indicate that the positions of the corresponding protons in the amino acid residues are determined exclusively via HOHAHA spectra; underlined chemical shifts refer to protons whose positions in the amino acid side chain were determined exclusively via NOESY spectra. $^3J_{HN\alpha}$ values are in Hertz.

exchange of the nearby fast exchanging O$^\zeta$H (for Tyr72 and Tyr108) or N$^{\epsilon 2}$H (for His32 and His83) proton. Three peaks at 11.06, 11.65, and 9.28 ppm involving the N$^{\epsilon 2}$H protons of His35 and His117 and the backbone NH of Lys18 are directly attributed to solvent exchange. The other resonances could not be unambiguously assigned. A second set of NOESY and ROESY experiments performed at 12 °C yielded an essentially identical set of cross peaks at the H_2O frequency and confirmed the assignment of the C$^\alpha$H proton of Lys52.

Of particular interest in the analysis of the protein hydration of azurin is whether any evidence can be found for NOE connectivities between a long-lived water molecule and the residues surrounding the crevice above His117. In the crystal structure of azurin [modified by the introduction of protons using the program QUANTA (Molecular Simulations Inc.)] several azurin protons are within a distance of 4 Å from water molecule W137. Therefore, they would be expected to exhibit NOE and ROE cross peaks at the water frequency. These protons include the C$^\epsilon$H and C$^\delta$H protons of Phe114 and the C$^{\epsilon 1}$H and C$^{\delta 2}$H protons of His117, which are at a distance from the water molecule of 2.84, 3.77, 3.78, and 3.72 Å, respectively (Figure 1). From an analysis of the 2D NOESY and ROESY spectra recorded with shaped-pulse suppression of the solvent resonance, it is possible to unambiguously establish the absence of any NOE or ROE cross peak that would correspond to a close approach of the histidine side

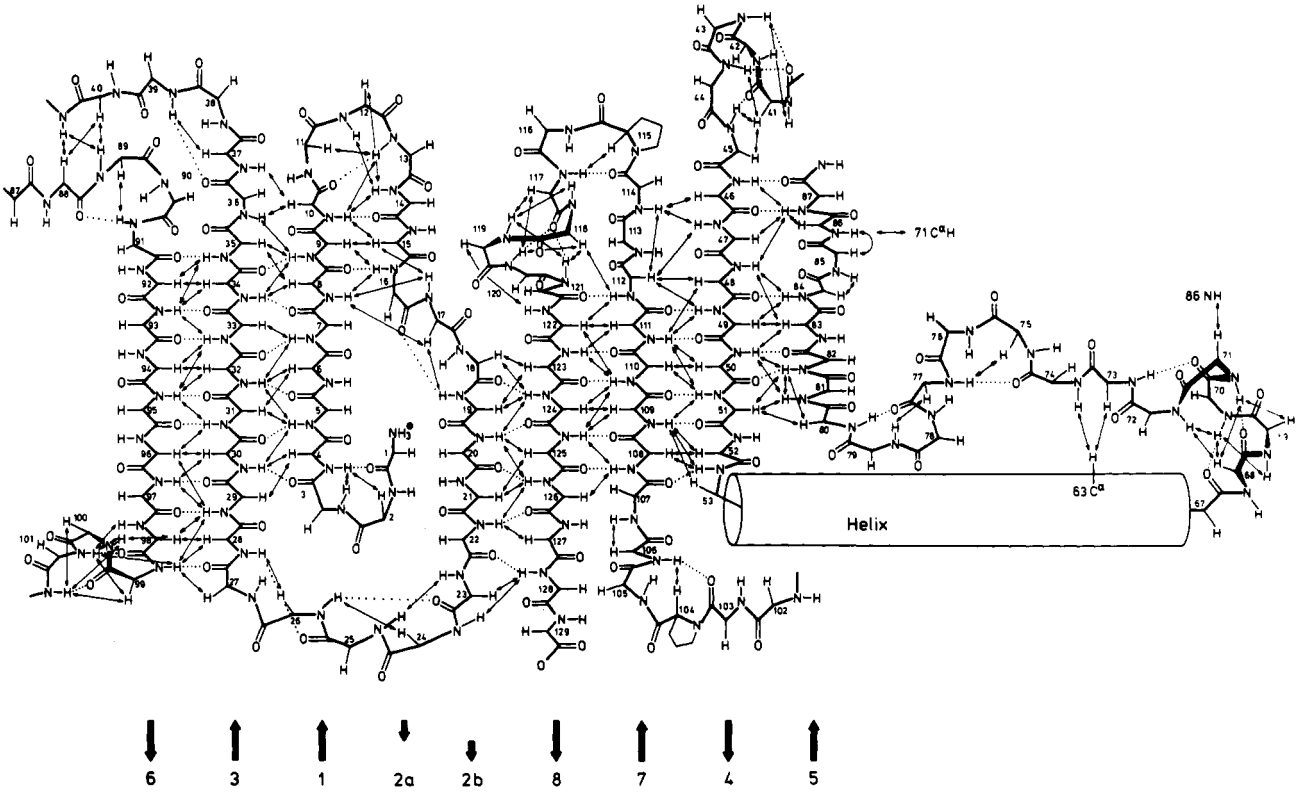

FIGURE 6: Schematic representation of the super secondary structure of azurin in solution. Arrows indicate experimentally observed long- and medium-range NOE connnectivities, and dotted lines are hydrogen bonds as extracted from the crystal structure. The numbering of β-strands is derived from the crystal structure (Baker, 1988).

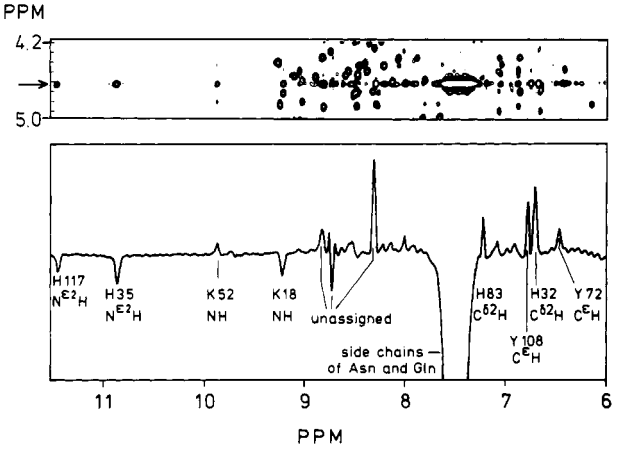

FIGURE 7: (Upper panel) Part of the 2D ROESY spectrum of azurin in 90% H_2O/10% D_2O at 25 °C. The arrow indicates the water frequency. (Lower panel) Cross section through the same spectrum along F_2 at the F_1 frequency of the water. Resonance assignments for selected peaks are indicated.

chain protons or the $C^{\delta}H$ proton of Phe114 to a long-lived water molecule. The $C^{\epsilon}H$ proton of Phe114 overlaps with the side chain amide peaks around 7.5 ppm.

DISCUSSION

The NMR analysis showed that the secondary structure and the molecular topology of *A. denitrificans* azurin in solution (Figure 6) are very similar to those observed in the crystal structure. There are minor differences due to different criteria for the definition of secondary structure elements. X-ray analysis identifies the α-helix as running from residues 55 to 67 and classifies the residues 52–55 as a 3_{10} helical turn. The NMR data show $d_{\alpha N}(i,i+4)$ NOE connectivities, which are characteristic for an α-helix, between residues 55 and 65. At both ends of this stretch the presence of $d_{\alpha N}(i,i+2)$ NOEs points to a 3_{10} helix. Taking into account the continuous $d_{\alpha N}(i,i+3)$ connectivities, the helix is defined as running from residue 53 to 67. The identification of tight turns on the basis of NOE connectivities is in accordance with the crystal structure (Figure 4).

Comparison of the secondary structure of *A. denitrificans* azurin with the structure of *Ps. aeruginosa* azurin (Van de Kamp et al., 1992) in solution as determined from NMR data shows that they are highly similar. This is in accordance with the high degree of similarity found for the crystal structures of the two azurins. The best-fit superposition of the two crystal structures gives a root mean square distance for the backbone atoms of residues 3–127 of 0.7 Å. The biggest differences between the two structures are some minor displacements of the polypeptide backbone in two loops (Gly67–Gln70 and Thr103–Glu106) and local differences around residues 36 and 40, due to the presence of two prolines in *Ps. aeruginosa* azurin at these positions (Nar et al., 1991a,b).

The availability of NMR assignments for many proteins has triggered renewed interest in the origin and calculation of chemical shifts. Wishart et al. (1991) have established a database of NMR proton assignments for 70 proteins with known 3D structures and found a strong correlation between chemical shifts of $C^{\alpha}H$ protons and secondary structure. This correlation is less pronounced for NH protons, and a reasonable correlation between H-bond energy and chemical shift is found instead. The high similarity of the chemical shifts of *Ps. aeruginosa* and *A. denitrificans* azurins confirms this finding. Residues 41–47 and 110–119, which are close to the copper site, have NH chemical shifts that are very different from random coil values in a pattern that may be very characteristic for azurins. A specific pattern is also found for residues around the copper site in three plastocyanins, but there the pattern is significantly different from that found for azurin, which is

in turn different from amicyanin (plots not shown) (Driscoll et al., 1987; Chazin et al., 1988; Moore et al., 1988; Lommen et al., 1991). We note that a comparison of chemical shifts for several "zinc fingers" similarly showed that the chemical shift of residues at specific positions could be used as a diagnostic tool for identifying the subclass of a zinc finger (Lee et al., 1992).

It is interesting to attempt to find a rationalization for the larger chemical shift differences between some of the backbone protons of *A. denitrificans* and *Ps. aeruginosa* azurins in terms of the respective crystal structures. A description of chemical shifts in protein NMR spectra has been proposed by several authors, in which proton chemical shifts can be divided into contributions from aromatic ring current effects, the magnetic anisotropy of nearby chemical bonds, and the polarization due to local electric fields (Williamson et al., 1991; Ösapay et al., 1991; Augspurger et al., 1992). Since the polypeptide backbone folds of the two azurins are very similar, the contribution from the magnetic anisotropy of peptide bonds should on the average cancel out. Therefore, the differences in chemical shifts between the backbone protons of the two azurins should be explained in the main by differences in the electric field and ring current effects. However, only in a few cases are the causes for chemical shift deviations larger than 0.5 ppm self-evident (Figure 5c,d). The difference of 1.04 and 1.24 ppm for NH protons of residues 19 and 37 can be accounted for by differences in H-bonding patterns as found in the crystal structures. In *A. denitrificans* azurin the $N^{\delta 1}$ atom of His35 forms a hydrogen bond to the NH proton of Gly37; in *Ps. aeruginosa* the protonated $N^{\delta 1}H$ forms a hydrogen bond to the main chain carbonyl O atom of residue 36. Likewise, the H-bond between the NH of residue 19 and the side chain of Thr17 in *Ps. aeruginosa* azurin cannot be formed with the side chain of Leu17 in *A. denitrificans* azurin (Nar et al., 1991a; Baker, 1988). The difference in $C^{\alpha}H$ chemical shifts for His35 (1.15 ppm) and the spatially close His46 (0.57 ppm) could be explained by the different states of protonation of His35. The chemical shift differences for residues 118 and 119 are probably due to the ring current shift effect from the tryptophan ring of residue 118. This residue is only present in *A. denitrificans* azurin.

Assuming that the chemical shift differences exhibit a Gaussian distribution, the precision by which the center value of the distribution can be estimated is given by the rmsw divided by the square root of the number of experimental points in the distribution. The mean difference in the random coil-corrected NH proton chemical shifts between the two azurins is found to be 0.00 (± 0.03) ppm. In contrast, the mean difference in random coil-corrected $C^{\alpha}H$ chemical shifts between the two azurins deviates significantly from zero, i.e., 0.09 (± 0.02) ppm. It is not clear what the origin of this effect might be. Buckingham (1960) has described the potential for extensive effects of charged and polar groups on the chemical shifts of solute molecules as well as the involvement of solvent effects. Figure 5 shows that the NH chemical shifts cover a broader range than the $C^{\alpha}H$ chemical shifts. The NH chemical shift is a delicate function of the H-bonding pattern, and the minute differences in H-bonds between the two azurins may obscure other effects. Therefore, a tentative explanation for the observation of the small bias for the $C^{\alpha}H$ chemical shifts may be sought in the difference in overall charge between the two azurins at the pH used for the experiments (pH 5.5) since reduced *Ps. aeruginosa* azurin has a pI of 4.7 whereas *A. denitrificans* has a pI of 7.9.

The high degree of similarity between the experimentally determined secondary structure and molecular topology of *A. denitrificans* azurin in solution and in the crystalline state (Baker, 1988) allows us to attempt to correlate other characteristics of the NMR spectrum of the protein in terms of the crystal structure. Three of the five histidine $N^{\epsilon 2}$ protons, from residues His35, His46, and His117, are observed in the NMR spectra. For the majority of solvent-exposed histidine residues, this proton is not usually observed because of rapid exchange with the solvent, as is the case here for His32 and His83. The copper ligand residue His46 is buried in the protein, and in the crystal structure its $N^{\epsilon 2}H$ is H-bonded to the main chain carbonyl group of Asn10 and is thus protected from rapid exchange with the solvent. Until recently, it was thought that His35 had a function in the electron transfer reaction of azurin with its redox partners, and a lot of attention was given to the difference in pH titration behavior between different azurins. A pH titration of *A. denitrificans* azurin followed with NMR spectroscopy showed that the side chain of His35 could not be protonated down to pH 4 (Groeneveld et al., 1988), suggesting that His35 is not accessible to the solvent. This is confirmed by the observation of the $N^{\epsilon 2}H$ proton in this study and supported by the crystal structure where both ring nitrogens of His35 are involved in H-bonding and are somewhat buried in the protein. The side chain of His35 in *Ps. aeruginosa* azurin has a slightly more solvent-accessible position in the protein and shows a normal titration behavior, and its $N^{\epsilon 2}H$ resonance is not observed in solution due to faster exchange with the solvent (Van de Kamp et al., 1992).

The observation that the $N^{\epsilon 2}H$ proton of His117 is in slow exchange with the solvent is less easily rationalized. In the crystal structure, the $N^{\epsilon 2}H$ proton of His117 is exposed to the solvent and not in contact with any protein atom. Instead, the histidine ring contacts a well-defined water molecule with low temperature factor (W137). This water molecule occupies a small pocket in the surface of the azurin molecule above His117 and is H-bonded to the $N^{\epsilon 2}H$ of His117 and the carbonyl oxygen of Ala43. It has been ascribed a potential role in forming part of the electron transfer pathway of azurin (Nar et al., 1991b). Analysis of the NOESY and ROESY spectra recorded with shaped-pulse selective suppression of the solvent yielded no evidence for the presence of a long-lived water molecule in the vicinity of the His117 side chain. Quantitatively, the observation of slow exchange of the His117 proton with solvent means that the lifetime of the $N^{\epsilon 2}H$ proton of His117 is of the order of milliseconds or more. The lack of observation of either NOE or ROE connectivities between protons lining the W137 pocket and solvent suggests that the residence time of any water molecule in that site (and likely H-bonded to His117) is shorter than the rotational correlation time of the azurin molecule, i.e., shorter than about 7 ns (Otting et al., 1991; Clore et al., 1990). Essentially identical characteristics have been observed in the slow solvent exchange of the $N^{\epsilon 2}H$ proton of His117 and the presence of a H-bond to a water molecule in the crystal structure of *Ps. aeruginosa* azurin (Van de Kamp et al., 1992; Nar et al., 1991a). It is interesting to compare the characteristics of the homologous copper coordinating histidine residue in other blue copper proteins. In the crystal structures of several plastocyanins, pseudo-azurin, and amicyanins, the $N^{\epsilon 2}H$ proton of the corresponding histidine ligands is also H-bonded to a water molecule (Guss & Freeman, 1983; Collyer et al., 1990; Petratos et al., 1988; Durley et al., 1993; Romero et al., 1994). However, in the NMR spectra of plastocyanins and amicyanin,

the concomitant $N^{\epsilon 2}H$ protons are not observed (Driscoll et al., 1987; Moore et al., 1988a; Chazin et al., 1988; Lommen et al., 1991).

For both plastocyanin and amicyanin in the reduced form, the histidine ligand corresponding to His117 of azurin is titratable: upon protonation of the histidine the copper coordination changes from a distorted tetrahedral to a trigonal arrangement (Guss et al., 1986; Lommen & Canters, 1990).

Based on the lack of evidence for a strong H-bond between the side chain of His117 and a water molecule, an alternative explanation must be sought for the slow exchange behavior of the His117 $N^{\epsilon 2}H$ proton in the two azurin molecules. A potential cause may be that, because of the side chain's direct participation in the coordination of the copper atom, the pK_a for protonation of His117 at the $N^{\delta 1}H$ proton is significantly decreased and thereby precludes efficient exchange of the $N^{\epsilon 2}H$ proton by an acid-catalyzed mechanism. Likewise, the pK_a of deprotonation at the $N^{\epsilon 2}H$ proton may be significantly increased to hamper base-catalyzed exchange (Englander & Kallenbach, 1984; Van de Kamp et al., 1992). However, the high similarity in the electronic structures of azurins, plastocyanins, and amicyanins would suggest that the pK_as of the homologous ligand histidines would also be similar, which is not observed experimentally. Alternatively, it may be that the architecture of the copper site and the coordinating residues in azurin does not lend itself to rapid reorganization, such as that seen in the pH-dependent coordination of the copper atom in the plastocyanins and amicyanins, as might be required during the proton exchange mechanism.

ACKNOWLEDGMENT

Drs. M. van de Kamp and A. P. Kalverda are thanked for valuable discussions.

REFERENCES

Adman, E. T. (1985) *Top. Mol. Struct. Biol. 6*, 1–42.
Adman, E. T. (1991) *Adv. Protein Chem. 42*, 145–197.
Armstrong, F. A., Driscoll, P. C., & Hill, H. A. O. (1985) *FEBS Lett. 190*, 242–248.
Aue, W. P., Bartholdi, E., & Ernst, R. R. (1976) *J. Chem. Phys. 64*, 2229–2246.
Augspurger, J., Pearson, J. G., Oldfield, E., Dykstra, C. E., Park, K. D., & Schwartz, D. (1992) *J. Magn. Reson. 100*, 342–357.
Baker, E. N. (1988) *J. Mol. Biol. 203*, 1071–1095.
Bax, A. (1989) *Methods Enzymol. 176*, 151–168.
Bax, A., Sklenar, V., Clore, G. M., & Gronenborn, A. M. (1987) *J. Am. Chem. Soc. 109*, 6511–6513.
Bax, A., Ikura, M., Lewis, E. K., Torchia, D. A., & Tschudin, R. (1990) *J. Magn. Reson. 86*, 304–318.
Bax, A., Ikura, M., Kay, L. E., & Zhu, G. (1991) *J. Magn. Reson. 91*, 174–178.
Bothner-By, A. A., Stevens, R. L., & Lee, J. (1984) *J. Am. Chem. Soc. 106*, 811.
Braunschweiler, L., & Ernst, R. R. (1983) *J. Magn. Reson. 53*, 521–528.
Buckingham, A. D. (1960) *Can. J. Chem. 38*, 300–307.
Canters, G. W., & Gilardi, G. (1993) *FEBS Lett. 325*, 39–48.
Chazin, W. J., Rance, M., & Wright, P. E. (1988) *J. Mol. Biol. 202*, 603–622.
Clore, G. M., Bax, A., Wingfield, P. T., & Gronenborn, A. (1990) *Biochemistry 29*, 5671–5676.
Collyer, C. A., Guss, J. M., Sugimura, Y., Yoshizaki, F., & Freeman, H. C. (1990) *J. Mol. Biol. 211*, 617–632.
Davis, D. G., & Bax, A. (1985) *J. Am. Chem. Soc. 107*, 2820–2821.
Den Blaauwen, T., & Canters, G. W. (1993) *J. Am. Chem. Soc. 115*, 1121–1129.
Derome, A. E., & Williamson, M. P. (1990) *J. Magn. Reson. 88*, 177–185.
Driscoll, P. C., Hill, H. A. O., & Redfield, C. (1987) *Eur. J. Biochem. 170*, 279–292.
Driscoll, P. C., Clore, G. M., Beress, L., & Gronenborn, A. M. (1989) *Biochemistry 28*, 2178–2187.
Driscoll, P. C., Clore, G. M., Marion, D., Wingfield, P. T., & Gronenborn, A. M. (1990) *Biochemistry 29*, 3542–3556.
Durley, R., Chen, L., Lim, W. W., Mathews, F. S., & Davidson, V. L. (1993) *Protein Sci. 2*, 739–752.
Englander, S. W., & Kallenbach N. R. (1984) *Q. Rev. Biophys. 16*, 521–655.
Groeneveld, C. M., & Canters, G. W. (1988) *J. Biol. Chem. 263*, 167–173.
Groeneveld, C. M., Ouwerling, M. C., Erkelens, C., & Canters, G. W. (1988) *J. Mol. Biol. 200*, 189–199.
Guss, J. M., & Freeman, H. C. (1983) *J. Mol. Biol. 169*, 521–563.
Guss, J. M., Harrowell, P. R., Murata, M., Norris, V. A., & Freeman, H. C. (1986) *J. Mol. Biol. 192*, 361–387.
He, S., Modi, S., Bendall, D. S., & Gray, J. C. (1991) *EMBO J. 10*, 4011–4016.
Hoitink, C. W. G., & Canters, G. W. (1992) *J. Biol. Chem. 267*, 13836–13842.
Jeener, J., Meier, B. H., Bachman, P., & Ernst, R. R. (1979) *J. Chem. Phys. 71*, 4546-4553.
Kalverda, A. P., Lommen, A., Wijmenga, S., Hilbers, C. W., & Canters, G. W. (1991) *J. Inorg. Biochem. 43*, 171.
Karlsson, B. G., Pascher, T., Nordling, M., Arvidsson, R. H. A., & Lundberg, L. G. (1989) *FEBS Lett. 246*, 211–217.
Karlsson, B. G., Nordling, M., Pascher, T., Tsai, L. C., Sjölin, L., & Lundberg, L. G. (1991) *Protein Eng. 4*, 343–349.
Kay, L. E., & Bax, A. (1990) *J. Magn. Reson. 86*, 110–126.
Kay, L. E., Marion, D., & Bax, A. (1989) *J. Magn. Reson. 84*, 72–84.
Kraulis, P. J. (1991) *J. Appl. Crystallogr. 24*, 946–950.
Lee, M. S., Mortishire-Smith, J., & Wright, P. E. (1992). *FEBS Lett. 309*, 29–33.
Light, P. A. P., & Garland, P. B. (1971) *Biochem. J. 14*, 123–134.
Live, D. H., Davis, D. G., Agosta, W. C., & Cowburn, D. (1984) *J. Am. Chem. Soc. 106*, 1939–1941.
Lommen, A., & Canters, G. W. (1990) *J. Biol. Chem. 265*, 2768–2774.
Lommen, A., Wijmenga, S., Hilbers, C. W., & Canters, G. W. (1991) *Eur. J. Biochem. 201*, 695–702.
Macura, S., Huang, Y., Suter, D., & Ernst, R. R. (1981) *J. Magn. Reson.* 43, 259–281.
Marion, D., & Wüthrich, K. (1983) *Biochem. Biophys. Res. Commun. 113*, 967–974.
Marion, D., Driscoll, P. C., Kay, L. E., Wingfield, P. T., Bax, A., Gronenborn, A. M., & Clore, G. M. (1989a) *Biochemistry 28*, 6150–6156.
Marion, D., Ikura, M., & Bax, A. (1989b) *J. Magn. Reson. 84*, 425–430.
Marion, D., Ikura, M., Tschudin, R., & Bax, A. (1989c) *J. Magn. Reson. 85*, 393–398.
Messerle, B. A., Wider, G., Otting, G., Weber, C., & Wüthrich, K. (1989) *J. Magn. Reson. 85*, 608–613.
Moore, J. M., Chazin, W. J., Powis, R., & Wright, P. E. (1988a) *Biochemistry 27*, 7806–7816.
Moore, J. M., Case, D. A., Chazin, W. J., Gippert, G. H., Havel, T. F., Powls, R., & Wright, P. E. (1988b) *Science 240*, 314–317.
Moore, J. M., Lepre, C. A., Gippert, G. P., Chazin, W. J., Case, D. A., & Wright, P. E. (1991) *J. Mol. Biol. 221*, 533–555.
Muchmore, D. C., McIntosh, L. P., Russell, C. B. Anderson, D. E., & Dahlquist, F. W. (1989) *Methods Enzymol. 177*, 44–73.
Nar, H., Messerschmidt, A., Huber, R., Van de Kamp, M., & Canters, G. W. (1991a) *J. Mol. Biol. 221*, 765–772.
Nar, H., Messerschmidt, A., Huber, R., Van de Kamp, M., & Canters, G. W. (1991b) *J. Mol. Biol. 218*, 427–447.

Nordling, M., Sigfridsson, K., Young, S., Lundberg, L. G., Hansson, O. (1991) *FEBS Lett. 291*, 327–330.
Norwood, T. J., Boyd, J., Heritage, J. E., Soffe, N., & Campbell, I. D. (1990) *J. Magn. Reson. 87*, 488–501.
Norwood, T. J., Crawford, D. A., Steventon, M. E., Driscoll, P. C., & Campbell, I. D. (1992) *Biochemistry 31*, 6285–6290.
Ösapay, K., & Case, D. A. (1991) *J. Am. Chem. Soc. 113*, 9436–9444.
Otting, G., & Wüthrich, K. (1989) *J. Am. Chem. Soc. 111*, 1871–1875.
Otting, G., Liepinsh, E., & Wüthrich, K. (1991) *Science 254*, 974–980.
Petratos, K., Dauter, Z., & Wilson, K. S. (1993) *Acta Crystallogr. B44*, 628–636.
Plateau, P., & Gueron, M. (1982) *J. Am. Chem. Soc.* 104, 7310–7311.
Rance, M., Sorensen, O. W., Bodenhausen, G., Wagner, G., Ernst, R. R., & Wüthrich, K. (1983) *Biochem. Biophys. Res. Commun. 117*, 479–485.
Romero, A., Hoitink, C. W. G., Nar, H., Messerschmidt, A., Canters, G. W. (1993) *J. Mol. Biol. 229*, 1007–1020.
Romero, A., Nar, H., Huber, R., Messerschmidt, A., Kalverda, A. P., & Canters, G. W. (1994) *J. Mol. Biol.* (in press).
Shaka, A. J., Keeler, J., Frenkiel, T., & Freeman, R. (1983) *J. Magn. Reson. 52*, 335–338.
Shaka, A. J., Lee, C. J., & Pines, A. (1988) *J. Magn. Reson. 77*, 274–293.
Shepard, W. E. B., Anderson, B. F., Lewandoski, D. A., Norris, G. E., & Baker, E. N. (1990) *J. Am. Chem. Soc. 112*, 7817–7819.
States, D. J., Haberkorn, R. A., & Ruben, D. J. (1982) *J. Magn. Reson. 48*, 286–292.
Sykes, A. G. (1991) *Adv. Inorg. Chem. 36*, 377–408.
Van de Kamp, M., Floris, R., Hali, F. C., & Canters, G. W. (1990a) *J. Am. Chem. Soc. 112*, 907–908.
Van de Kamp, M., Silvestrini, M. C., Brunori, M., Van Beeumen, J., Hali, F. C. & Canters, G. W. (1990b) *Eur. J. Biochem. 194*, 109–118.
Van de Kamp, M., Hali, F. C., Rosato, N., Finazzi Agro, A., & Canters, G. W. (1990c) *Biochim. Biophys. Acta 1019*, 293–292.
Van de Kamp, M., Canters, G. W. Wijmenga, S. S. Lommen, A., Hilbers, C. W., Nar, H., Messerschmidt, A., & Huber, R. (1992) *Biochemistry 31*, 10194–10207.
Williamson, M. P., & Asakura, T. (1991) *J. Magn. Reson. 94*, 557–562.
Wishart, D. S., Sykes, B. D., & Richards, F. M. (1991) *J. Mol. Biol. 222*, 311–333.
Wüthrich, K. (1986) *NMR of Proteins and Nucleic Acids*, Wiley, New York.